Eur. Phys. J. Special Topics 159, 27–36 (2008)

DOI: 10.1140/epjst/e2008-00690-2

THE EUROPEAN PHYSICAL JOURNAL SPECIAL TOPICS

Test of quantum mechanics by neutron interferometry

H. Rauch

Atominstitut der Österreichischen Universitäten, 1020 Wien, Austria

Abstract. Interferometry with massive elementary particles combines particle and wave features in a direct way. In this respect, neutrons are proper tools for testing quantum mechanics because they are massive, they couple to electromagnetic fields due to their magnetic moment, and they are subject to all basic interactions, and they are sensitive to topological effects, as well. They play a pionieering role in the development of interferometry with even heavier objects, like atoms, molecules and clusters. Deterministic and stochastic partial absorption experiments can be described by Bell-type inequalities. Recent neutron interferometry experiments based on postselection methods renewed the discussion about quantum nonlocality and the quantum measuring process. It has been shown that interference phenomena can be revived even when the overall interference pattern has lost its contrast. This indicates persisting coupling in phase space even in cases of spatially separated Schrödinger cat-like situations. These states are extremely fragile and sensitive to any kind of fluctuations or other decoherence processes. More complete quantum experiments also show that a complete retrieval of quantum states behind an interaction region becomes impossible in principle. The transition from a quantum world to a classical one is still an open question and will be tackled by means of dedicated decoherence experiments. Recent measurements deal with quantum contextuality and quantum state reconstruction. The observed results agree with quantum mechanical laws and may stimulate further discussions about their interpretations.

1 Introduction – basic relations

The perfect crystal neutron interferometer – first tested in 1974 at our 250 kW TRIGA reactor [1] – provides the highest intensity and became the most frequently used neutron interferometer due to its wide beam separation and its universal availability for fundamental, nuclear and solid-state physics [2]. It represents a macroscopic quantum device with characteristic dimensions of several centimeters (Fig. 1).

The basis for this kind of neutron interferometry is provided by the undisturbed arrangement of atoms in a monolithic perfect silicon crystal. An incident beam is split coherently at the first crystal plate, reflected at the middle plate and coherently superposed at the third plate. From general symmetry considerations it follows immediately that the wave functions in both beam paths, which compose the beam in the forward direction behind the interferometer, are equal ($\psi_0^{\mathrm{I}} = \psi_0^{\mathrm{II}}$), because they are transmitted-reflected-reflected (TRR) and reflected-reflected-transmitted (RRT), respectively. The theoretical treatment of the diffraction process from the perfect crystal is described by the dynamical diffraction theory [3]. To preserve the interference properties over the length of the interferometer, the dimensions of the monolithic system have to be accurate on a scale comparable to the so-called Pendellösung length ($\sim 50\,\mu$m). The whole interferometer crystal has to be placed on a stable goniometer table under conditions avoiding temperature gradients and vibrations. A phase shift between the two coherent beams

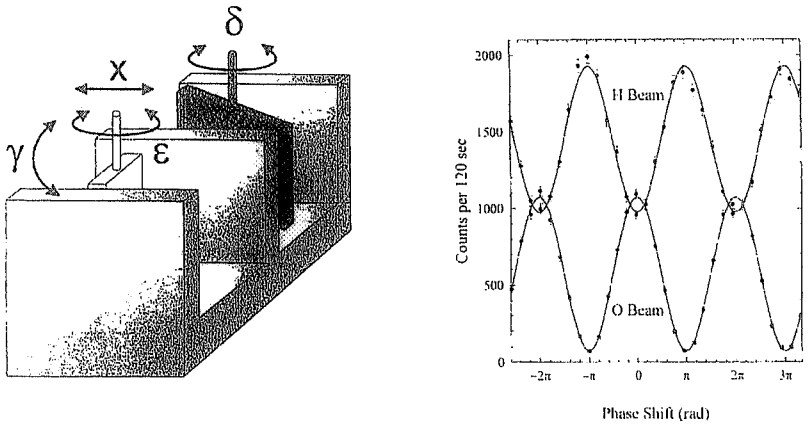

Fig. 1. Sketch of a symmetric perfect crystal neutron interferometer and a typical interference pattern.

can be produced by nuclear, magnetic or gravitational interactions. In the first case, the phase shift is most easily calculated using the index of refraction [4]:

$$n = \frac{k}{k_0} = 1 - \frac{\lambda^2 N}{2\pi}\sqrt{b_c^2 - \left(\frac{\sigma_r}{2\lambda}\right)^2} + i\frac{\sigma_r N\lambda}{4\pi} \cong 1 - \lambda^2\frac{Nb_c}{2\pi}, \tag{1}$$

where b_c is the coherent scattering length, σ_r the reaction cross-section, λ the wavelength of the neutrons, and N is the particle density of the phase-shifting material. The different k vector inside the phase shifter causes a spatial shift, $\vec{\Delta}$, of the wave packet which depends on the orientation of the sample surface, $\hat{s}$, its thickness D, and which is related to the scalar phase shift, χ, by

$$\psi \to \psi_0 e^{i\vec{\Delta}\cdot\vec{k}} = \psi_0 e^{-iNb_c\lambda D} = \psi_0\, e^{i\chi}, \tag{2}$$

where χ can be written as a path integral of the canonical momentum, k_c, along the beam paths, $\chi = \oint \vec{k}_c d\vec{s}$. Therefore, the intensity behind the interferometer becomes

$$I_0 \propto \left|\psi_0^I + \psi_0^{II}\right|^2 \propto (1 + \cos\chi)\,. \tag{3}$$

The intensity of the beam in the deviated direction, I_H, follows from particle conservation $I_0 + I_H = \text{const}$. Thus, the intensities behind the interferometer vary as a function of the thickness, D, of the phase shifter, the particle density, N, and the neutron wavelength, λ.

Neutron optics is a part of quantum optics, and many phenomena can be described properly in that terminology, where the coherence function plays an important role [5,6],

$$\Gamma(\vec{\Delta}) = \langle\psi(0)\psi(\vec{\Delta})\rangle, \tag{4}$$

which is the autocorrelation function of the wave function. Using a wave packet description for the wave functions (amplitudes $a(\vec{k})$)

$$\psi(\vec{x}) \quad \propto \quad \int a(\vec{k})\, e^{i\vec{k}\vec{x}}\, dk. \tag{5}$$

one obtains

$$I_0(\Delta_0) \propto \left|\psi_0^I + \psi_0^{II}\right|^2 \propto 1 + \left|\Gamma(\Delta_0)\right| \cos\chi_0 = 1 + |\Gamma(\Delta_0)|\cos(\vec{\Delta}_0 \cdot \vec{k}_0), \tag{6}$$

where Δ_0 and χ_0 denote the phase shifts related to the mean momentum, $\vec{k}_0$. This gives:

$$\left|\Gamma\left(\vec{\Delta}\right)\right| \propto \left|\int g\left(\vec{k}\right) e^{i\vec{k}\cdot\vec{\Delta}} d^3\vec{k}\right|. \tag{7}$$

Table 1. Properties of neutrons.

PARTICLE PROPERTIES		WAVE PROPERTIES
$m = 1.6748220(25) \times 10^{-27}$ kg	CONNECTION	$\lambda_c = \frac{h}{m.c} = 1.319695(20) \times 10^{-15}$ m
$s = \frac{1}{2}\hbar$	de Broglie	
$\mu = -9.6491783(18) \times 10^{-27}$ J/T	$\lambda_B = \frac{h}{m.v}$	for thermal neutrons: $\lambda = 1.8$ A, $v = 2200$ m/s
$\tau = 882.6(2.7)$ s	Schrödinger	$\lambda_B = \frac{h}{m.v} = 1.8 \times 10^{-10}$ m
$R = 0.7$ fm	$H\psi\left(\vec{r},t\right) = i\hbar\frac{\delta\psi\left(\vec{r},t\right)}{\delta t}$	$\Delta_c = \frac{1}{2\delta k} \cong 10^{-8}$ m
$\alpha = 12.0(2.5) \times 10^{-4}$ fm^3	&	$\Delta_p = v.\Delta t \cong 10^{-2}$ m
u - d - d - quark structure	boundary conditions	$\Delta_d = v.\tau = 1.942(5) \times 10^6$ m
		$0 \leq \chi \leq 2\pi(4\pi)$
m mass, s spin, μ magnetic moment, τ β-decay lifetime, R (magnetic) confinement radius, α electric polarizability; all other measured quantities like electric charge magnetic monopole and magnetic dipole moment are compatible with zero.	-μB ---------- ↕ two level system μB ----------	λ_c Compton wavelength, λ_B de Broglie wavelength, Δ_c coherence length, Δ_p packet length, δk momentum width, Δt chopper opening time, v group velocity, χ phase.

Thus the absolute value of the coherence function can be obtained from the fringe visibility, $|\Gamma(\vec{\Delta})| = (I_{max} - I_{min})/(I_{max} + I_{min})$, or as the Fourier transform of the momentum distribution, $g(\vec{k}) = |a(\vec{k})|^2$.

The mean square distance related to $|\Gamma(\vec{\Delta})|$ defines the coherence length, Δ_i^c which is for Gaussian distribution functions directly related to the minimum uncertainty relation ($\Delta_i^c \delta k_i = 1/2$). Similar relations can be obtained for time-dependent phenomena, where the spectral distribution, $g(\omega)$, and the temporal coherence function come into play.

Any experimental device deviates from the idealized situations: the perfect crystal can have slight deviations from its perfectness, and its dimensions may vary slightly; the phase shifter contributes to such deviations by variations in its thickness and inhomogeneities; and even the neutron beam itself contributes to a deviation from the idealized situation because of its momentum spread, δk. Therefore, the experimental interference patterns have to be described by a generalized relation,

$$I \propto A + B|\Gamma(\vec{\Delta})| \cos(\chi + \Phi_0), \tag{8}$$

where A, B and Φ are characteristic parameters of a certain set-up. It should be mentioned, however, that the idealized behaviour described by (3) can be nearly approached almost by a well-balanced set-up (Fig. 1). Phase shifts can be applied in the longitudinal, transverse and vertical directions, and the related coherence properties can be measured [7]. In the transverse direction the phase shift becomes wavelength independent ($\chi_T = -2d_{hkl}Nb_cD_0$; d_{hkl}: lattice distance), which implies a much larger coherence length in that direction.

All the results of interferometric measurements obtained up to now can be well explained in terms of the wave picture of quantum mechanics and the complementarity principle of standard quantum mechanics. Nevertheless, one should bear in mind that the neutron also carries well-defined particle properties, which have to be transferred through the interferometer. These properties are summarized in Table 1 together with a formulation in the wave picture. Both particle and wave properties are well established, and, therefore, neutrons seem to be a proper tool for testing quantum mechanics with massive particles, where the wave-particle dualism becomes very obvious.

All neutron interferometric experiments pertain to the case of self-interference, where during a certain time interval, only one neutron is inside the interferometer, if at all. Usually, at that time the next neutron has not yet been born and is still contained in the uranium nuclei

of the reactor fuel. Although there is no interaction between different neutrons, they have a certain common history within predetermined limits which are defined, e.g., by the neutron moderation process, by their movement along the neutron guide tubes, by the monochromator crystal and by the special interferometer set-up. Therefore, any interferometer pattern contains single particle and ensemble properties together.

2 Classic neutron interference experiments

There is no space to describe all classic neutron interference experiments in detail, they should be mentioned only. A comprehensive treatment can be found in [1].

- Gravity effects and noninertial frame phenomena measurements
  Here the action of ordinary gravity [8] of the Earth rotation [9] and the neutron Fizeau effect [10] have been demonstrated.
- 4π-spinor symmetry and spin-superposition experiments
  The first direct verification of the 4π-symmetry effect happened with neutrons [11,12], the spin-superposition principle has also been demonstrated on a macroscopic scale with neutrons [13,14]. Related experiments have dealt with the magnetic Josephson effect [15] and with multiphoton exchange within oscillating magnetic fields [16].

3 Decoherence and dephasing effects

3.1 Stochastic versus deterministic beam path detection

Neutrons can be absorbed in nuclei forming a compound nucleus which decays in most cases by γ-radiation, which can be detected easily with a high efficiency. Thus, an absorption process in one beam path denotes a beam path detection which cannot be retrieved since the compound nucleus acts as a system with a nearly infinite number of degrees of freedom.

A certain amount of beam attenuation can be achieved either by a semi-transparent material or by a proper chopper or slit system. The attenuation probability in the first case is defined by the attenuation cross section, σ_a, of the material [$\underline{a} = I/I_0 = \exp(-\sigma_a N D)$]. The change of the wave function is obtained directly from the complex index of refraction (eq. (1)):

$$\psi \to \psi_0 e^{i(n-1)kD} = \psi_0 e^{i\chi} e^{-\sigma_a N D/2} = e^{i\chi}\sqrt{\underline{a}}\psi. \tag{9}$$

Therefore, the beam modulation behind the interferometer is obtained in the following form

$$I_0 \propto \left|\psi_0^{I} + \psi_0^{II}\right|^2 \propto (1 + \underline{a}) + 2\sqrt{\underline{a}}\cos\chi. \tag{10}$$

On the other hand, the transmission probability of a chopper wheel or another shutter system is given by the open-to-closed ratio, $\underline{a} = t_{open}/(t_{open} + t_{closed})$, and one obtains after straightforward calculations

$$I \propto \left[(1 - \underline{a})\left|\psi_0^{II}\right|^2 + \underline{a}\left|\psi_0^{I} + \psi_0^{II}\right|^2\right] \propto (1 + \underline{a}) + 2\underline{a}\cos\chi, \tag{11}$$

i.e. the contrast of the interference pattern is proportional to $\sqrt{\underline{a}}$ in the first case and proportional to $\underline{a}$ in the second case, although the same number of neutrons are absorbed in both cases. The measured contrast lies along the lines "stochastic" and "deterministic" in Fig. 2 [16,17]. The different contrast becomes especially obvious for low transmission probabilities. The difference diverges for $\underline{a} \to 0$ but it has been shown that in this regime the variations of the transmission due to variations of the thickness or of the density of the absorber plate have to be taken into account which shifts the points below the $\sqrt{\underline{a}}$ ("stochastic") curve [18,19].

The region between the linear and the square-root behaviour can be reached by using very narrow chopper slits or narrow transmission lattices, where one starts to lose information

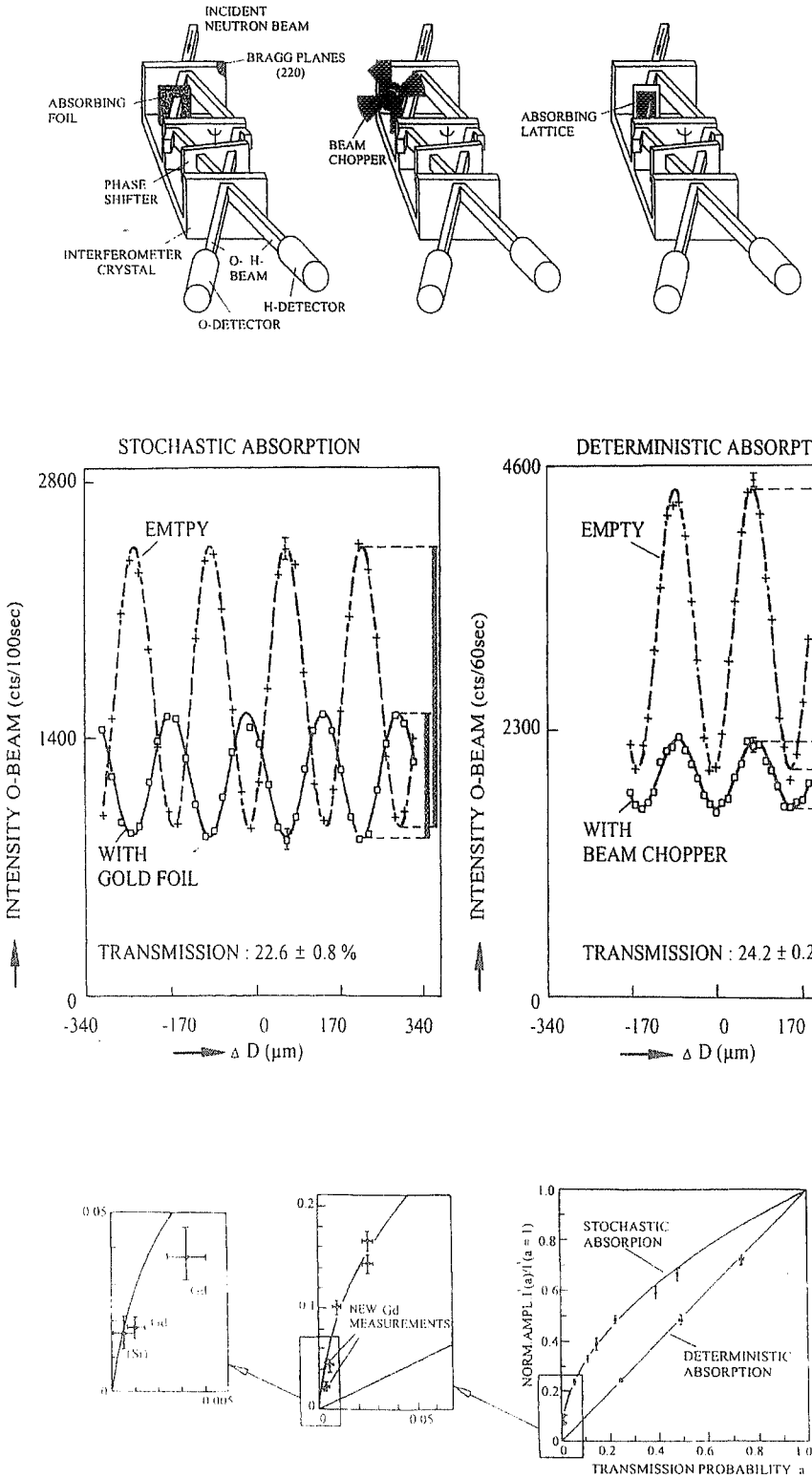

Fig. 2. Stochastic and deterministic absorption within the neutron interferometer.

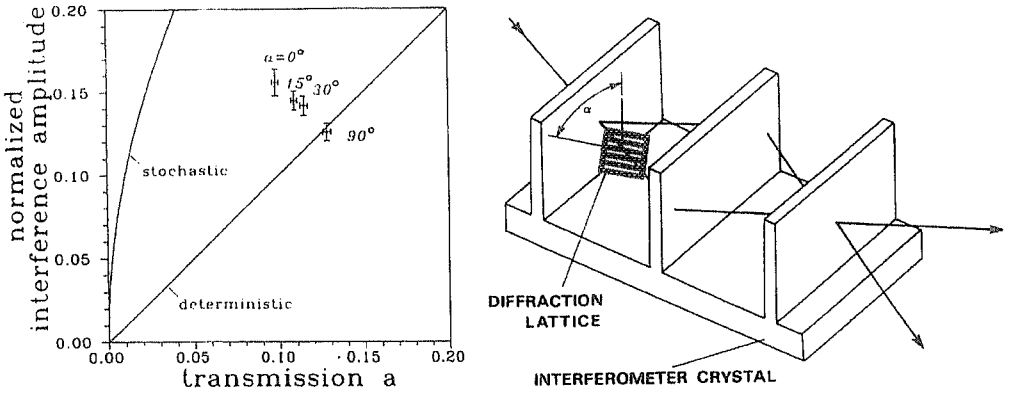

Fig. 3. Lattice absorber in the interferometer approaching the classical limit when the slits are oriented horizontally and the quantum limit when they are oriented vertically [17].

regarding through which individual slit the neutron went. This is exactly the region which shows the transition between a deterministic and a stochastic situation and, therefore, it can be formulated using a Bell-like inequality ($\sqrt{\underline{t}} > x > \underline{t}$) [20].

The stochastic limit corresponds to the quantum limit where one does no longer know through which individual slit the neutron went. A homogeneous absorber sheet, as discussed in the "stochastic" case before, gives the extreme case where one does not know which individual nucleus absorbed the neutron. Which situation exists depends on how the slit width, l, compares with the coherence lengths in the related direction. When the slit widths become comparable to the coherence lengths, the wave function behind the slits show distinct diffraction peaks which correspond to new quantum states ($n \neq 0$). The creation of the new quantum states means that those labeled neutrons carry information about the chosen beam path and, therefore, do not contribute to the interference amplitude [20] (Fig. 3). The diffraction effect from the lattice becomes maximal when it is oriented vertically ($\alpha = 0$), since the coherence length in the horizontal plane is rather large ($\sim 20\,\mu$m) due to the Bragg diffraction from the silicon crystal [21]. The situation reminds one of the transmission of a frisbee disk through a fence. A related experiment has been carried out by rotating an absorption lattice around the beam axis, where one changes from $l \ll \Delta_x{}^c$ (vertical slits) to $l \gg \Delta_y{}^c$ (horizontal slits). Thus, the attenuation factor a has to be generalized to include not only nuclear absorption and scattering processes but also lattice diffraction effects if they remove neutrons from the original phase space.

The partial absorption and coherence experiments are closely connected to the quantum duality principle, which states that the observation of an interference pattern and the acquisition of which-way informations are mutually exclusive. Various inequalities have been formulated to describe this mutual exclusion principle [22,23]. The most concise formulation reads as

$$V^2 + P^2 = \leq 1 \qquad (12)$$

where V denotes the fringe visibility (eq. (7)) and P is the predictability of the way through the interferometer, which is a quantitative measure of the a priori which-way knowledge.

A dedicted experiment using a double loop interferometer has been used to verify eq. (12) (see Fig. 4). In this case the fringe visibility within the second interferometer loop and the predictability are determined by the which-way probabilities w_I and w_{II} [24,25]

$$V = \frac{2\sqrt{w_I w_{II}}}{w_I + w_{II}} V_i, \quad P = |w_I - w_{II}|, \qquad (13)$$

with $w_{I,II} = \frac{N_{I,II}}{N_I + N_{II}}$.

w_I and w_{II} can be measured by blocking beam II or beam I, alternatively. V_i denotes the intrinsic visibility of the interferometer. w_I and w_{II} can be controlled by a phase shifter (a) in

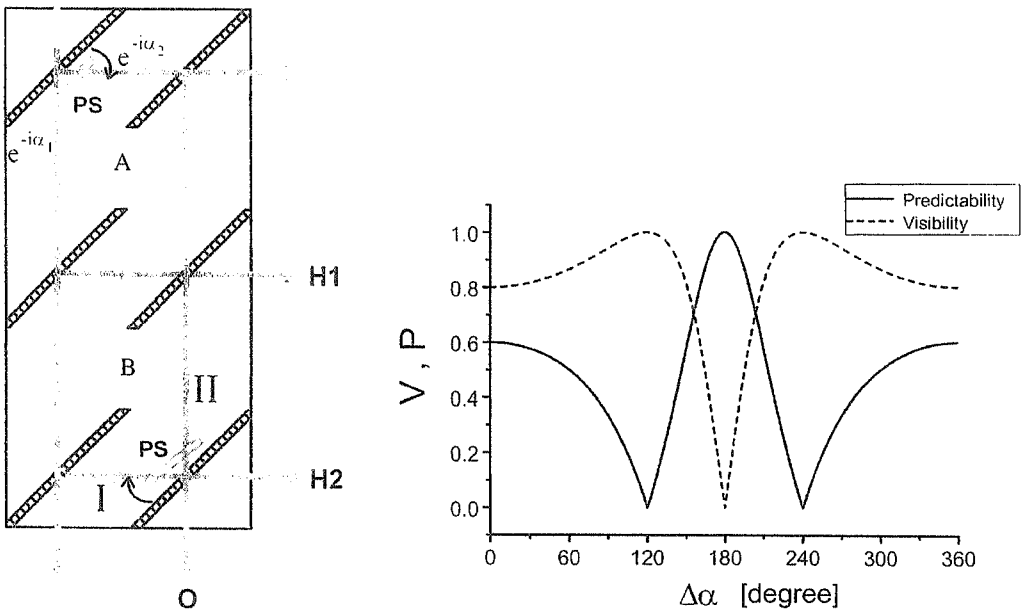

Fig. 4. Double loop interferometer and calculated fringe visibility and which-way predictability [24,25].

loop A and V can be measured by means of the phase shifter within loop B.

$$P = \left|\frac{1-2(1+\cos\alpha)}{1+2(1+\cos\alpha)}\right|, \quad V = \left|\frac{4\cos\frac{\alpha}{2}}{3+2\cos\alpha}\right|. \tag{14}$$

The measured results agree fairly well with the theoretical predictions supporting a value $P^2 + V^2 \leq 0.7$ [24,25]. The deviation from unity is caused by the nonperfect contrast within the loops A and B. It should be mentioned that these quantum phenomena can be used to establish a kind of homodyne detection of neutrons [26].

3.2 Dephasing by magnetic noise fields

Neutrons couple due to their magnetic moment to any kind of magnetic fields. When static or time-dependent resonance or single mode fields are applied, the typical 4π-symmetry and spin-superposition phenomena can be observed [11–16]. Magnetic noise fields applied onto the coherent beams cause a partial spin reversal and photon exchanges between the neutron and the noise field, which causes a reduction of the fringe visibility at low order and a smearing effect of the momentum modulation at high order [27]. This photon exchange, which results also in a slight change of the energy of the neutron, occurs at all frequencies whereby the probabilities for single and multiphoton exchange are quite different [28]. Figure 5 shows the set-up and the results when a noise field has been applied onto beam paths I, or II, or the same noise fields onto both beam paths, simultaneously. The reduction of the visibility indicates a disturbance of the overall coherence of both beams but its recovery when applied to both beams demonstrate that full coherence can be retrieved, which means that even the photon exchanges become reversible. This indicates that coherence can preserved even in cases when the visibility becomes reduced but the interaction Hamiltonian is at least still known in principle. Whether that holds for all frequency ranges has to be investigated in detail. A critical limit may occur when the time variations reach a value comparable to the coherence time of the beam of about 1 ns. The

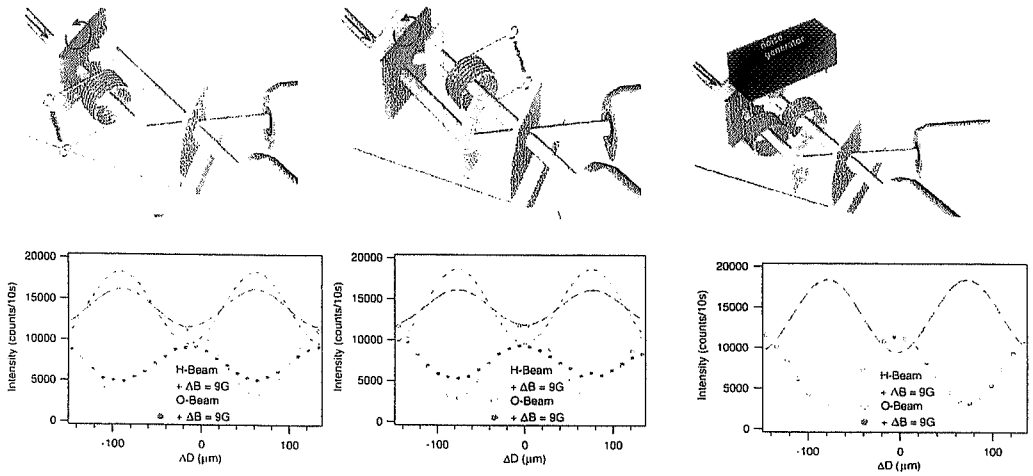

Fig. 5. Loss of contrast due to magnetic noise fields (left and middle) and no loss of contrast when the same noise field is applied to both coherent beams (right) [27].

recently developed method of a complete density matrix measurement may be useful to shed more light onto the question how a quantum system transforms into a classical system [29].

The question of decoherence plays also an important role in connection with quantum communication and quantum computing. When atoms or molecules are used as quantum objects many more degrees of freedom contribute to decoherence effects (e.g. [30]). With neutrons these effects can be treated individually. Speculations whether the geometric phases are more robust against decoherence effects are under investigation.

4 Quantum contextuality

A. Einstein, B. Podolsky and N. Rosen [31] argued that quantum mechanics may not be complete since non-local correlations between spatially separated systems are predicted, which stimulated the discussion about "hidden" variables and a more "realistic" theory. J. Bell [20] formulated inequalities which can decide between the quantum mechanical and the "realistic" view. Related experiments with entangled photons verified the non-local view of quantum mechanics [32–34]. Entanglement does not exist between different entities (photons) only but also between different degrees of freedom of a single system (neutron). This yields the concept of "contextuality", which states that independent measurements of independent observables are correlated. In our case the beam path through the interferometer and the spin states are taken as independent observables. In this case a Bell-like inequality can be formulated, which can be measured from the counting rates N at different values of the phase shift χ and the spin rotation angle α [35,36].

$$
\begin{aligned}
&-2 \leq \mathrm{S} \leq 2, \\
&\mathrm{S} = \mathrm{E}(\alpha_1, \chi_1) + \mathrm{E}(\alpha_1, \chi_2) - \mathrm{E}(\alpha_2, \chi_1) + \mathrm{E}(\alpha_2, \chi_2), \\
&\mathrm{E}(\alpha, \chi) = \frac{\mathrm{N}(\alpha, \chi) + \mathrm{N}(\alpha + \pi, \chi + \pi) - \mathrm{N}(\alpha, \chi + \pi) - \mathrm{N}(\alpha + \pi, \chi)}{\mathrm{N}(\alpha, \chi) + \mathrm{N}(\alpha + \pi, \chi + \pi) + \mathrm{N}(\alpha, \chi + \pi) + \mathrm{N}(\alpha + \pi, \chi)}.
\end{aligned} \tag{15}
$$

The maximal violation of this inequality due to quantum mechanics happens for the following parameters: $\alpha_1 = 0$, $\alpha_2 = \pi/2$, $\chi_1 = \pi/4$ and $\chi_2 = -\pi/4$ and amounts to $\mathrm{S} = 2\sqrt{2} = 2.82$.

The measurement scheme is shown in Fig. 6. The precise determination of the related counting rates at the parameter values given above yielded a value for S of [36]:

$$\mathrm{S} = 2.051 \pm 0.019,$$

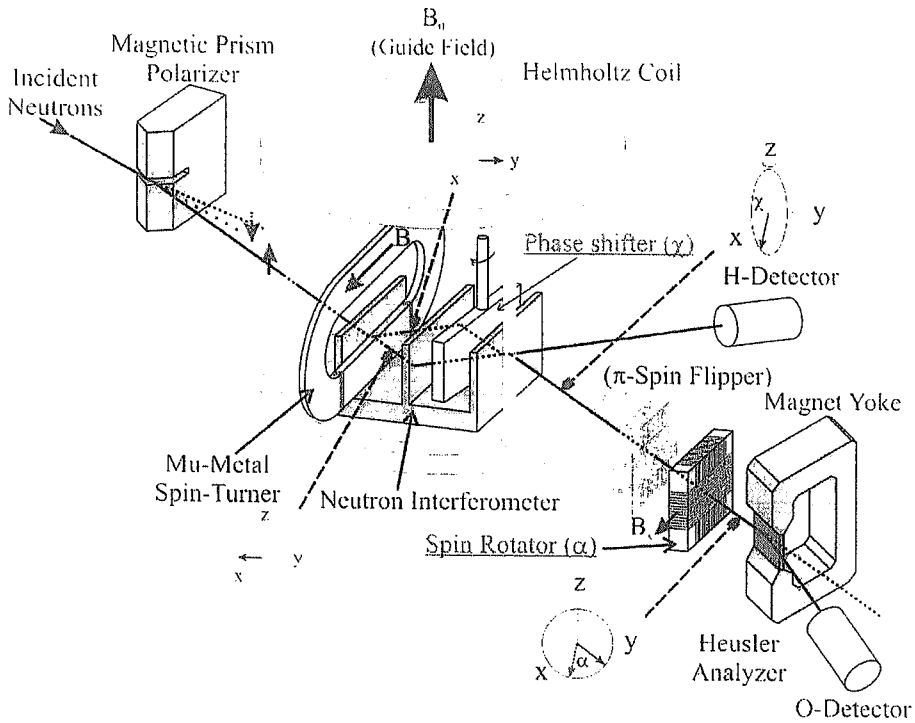

Fig. 6. Sketch of the experimental setup for the contextuality experiment. The phase χ and the direction of polarization α could be varied independently [36].

which is within a 3σ-limit above two, verifying, for the first time, the contextuality principle of quantum mechanics. The maximal violation of $S = 2.82$ has not been achieved because the contrast of the interference pattern and the neutron polarization were below unity. These quantities play in this kind of measurements a similar role as the finite efficiency of the photon detectors in entangled photon experiments.

5 Discussion

Decoherence and the appearance of a classical world in quantum mechanics was the main topic of this contribution to the conference. It has been shown that neutrons are a proper tool to tackle this question by means of neutron interferometry experiments. Several partial beam absorption experiments have been discussed in terms of wave-particle duality, where an inequality relating fringe visibility and path distinguishability has been tested. In this case no retrieval of a which-way detection seems to be feasible, indicating real decoherencing. On the other hand, a loss of contrast caused by magnetic noise fields can be retrieved when the same noise field is applied to both coherent beams of a Mach-Zehnder interferometer. In this case not only the same spin direction has to be recovered but also the related multiphoton exchange has to be balanced. In order to demonstrate that in all quantum states more information is available than usually extracted is demonstrated by means of recent contextuality experiments, where it has been shown that there exists also entanglement between external and internal degrees of freedom.

Most of the experimental work has been supported by projects of the Austrian Science Foundation (FWF), most recently by the project SFB1513.

References

1. H. Rauch, W. Treimer, U. Bonse, Phys. Lett. A **47**, 369 (1974)
2. H. Rauch, S.A. Werner (eds.), *Neutron Interferometry* (Clarendon Press, Oxford, 2000)
3. H. Rauch, D. Petrascheck, *Neutron Diffraction*, edited by H. Dachs, Chap. 9 (Springer Verlag, Berlin, 1978)
4. V.F. Sears, *Neutron Optics* (Oxford University Press, Oxford, 1989)
5. R.J. Glauber, Phys. Rev. **130**, 2529; Phys. Rev. **131**, 2766 (1963)
6. L. Mandel, E. Wolf, *Optical Coherence and Quantum Optics* (Cambridge University Press, 1995)
7. H. Rauch, H. Wölwitsch, H. Kaiser, R. Clothier, S.A. Werner, Phys. Rev. A **53**, 902 (1996)
8. R. Colella, A.W. Overhauser, S.A. Werner, Phys. Rev. Lett. **34**, 1472 (1975)
9. S.A. Werner, J.L. Staudenmann, R. Colella, Phys. Rev. Lett. **42**, 1103 (1979)
10. A.G. Klein, G.I. Opat, A. Cimmino, A. Zeilinger, W. Treimer, R. Gähler, Phys. Rev. Lett. **46**, 1551 (1981)
11. H. Rauch, A. Zeilinger, G. Badurek, A. Wilfing, W. Bauspiess, U. Bonse, Phys. Lett. A **54**, 425 (1975)
12. S.A. Werner, R. Colella, A.W. Overhauser, C.F. Eagen, Phys. Rev. Lett. **35**, 1053 (1975)
13. J. Summhammer, G. Badurek, H. Rauch, U. Kischko, A. Zeilinger, Phys. Rev. A **27**, 2523 (1983)
14. G. Badurek, H. Rauch, J. Summhammer, Phys. Rev. Lett. **51**, 1015 (1983)
15. G. Badurek, H. Rauch, D. Tuppinger, Phys. Rev. A **34**, 2600 (1986)
16. J. Summhammer, K.A. Hamacher, H. Kaiser, H. Weinfurter, D.L. Jacobson, S.A. Werner, Phys. Rev. Lett. **75**, 3206 (1995)
17. J. Summhammer, H. Rauch, D. Tuppinger, Phys. Rev. A **36**, 4447 (1987)
18. H. Rauch, J. Summhammer, M. Zawisky, E. Jericha, Phys. Rev. A **42**, 3726 (1990)
19. M. Namiki, S. Pascazio, Phys. Lett. A **147**, 430 (1990)
20. J.S. Bell, Physics **1**, 195 (1965)
21. H. Rauch, J. Summhammer, Phys. Rev. **46**, 7284 (1992)
22. W.K. Wooters, W.H. Zurek, Phys. Rev. D **19**, 473 (1979)
23. B.-G. Englert, Phys. Rev. Lett. **77**, 2154 (1996)
24. M. Zawisky, M. Baron, R. Loidl, Phys. Rev. A **66**, 063608 (2002)
25. M. Zawisky, Found. Phys. Lett. **17**, 561 (2004)
26. M. Suda, H. Rauch, M. Peev, J. Opt. B: Quantum Semiclass. Opt. **6**, 345 (2004)
27. M. Baron, *Messung von Quantenzuständen im Neutroneninterferometer*, Doctoral Thesis, TU Wien, 2005
28. J. Summhammer, K.A. Hamacher, H. Kaiser, H. Weinfurter, D.L. Jacobson, S.A. Werner, Phys. Rev. Lett. **75**, 3206 (1995)
29. Y. Hasegawa, J. Klepp, S. Filipp, R. Loidl (in preparation)
30. L. Hackermüller, K. Hornberger, B. Brezger, A. Zeilinger, M. Arndt, Nature **427**, 711 (2004)
31. A. Einstein, B. Podolsky, N. Rosen, Phys. Rev. **47**, 777 (1935)
32. A. Aspect, P. Grangier, G. Roger, Phys. Rev. Lett. **49**, 91 (1982)
33. Z.Y. Ou, L. Mandel, Phys. Rev. Lett. **61**, 50 (1988)
34. G. Weihs, T. Jennewein, C. Simon, H. Weinfurter, A. Zeilinger, Phys. Rev. Lett. **81**, 5039 (1998)
35. S. Basu, S. Bandyopadhyay, G. Kar, D. Home, Phys. Lett. A **279**, 281 (2001)
36. Y. Hasegawa, R. Loidl, G. Badurek, M. Baron, H. Rauch, Nature **425**, 46 (2003)